

Recombinant Human BMP-2 Enhances the Effects of Materials Used for Reconstruction of Large Cranial Defects

Mohammed E. Elsalanty, MD,* Yong-Chen Por, MBBS, MMed,†
David G. Genecov, MD,‡ Kenneth E. Salyer, MD,§
Qian Wang, PhD,|| C.R. Barcelo, MD,¶ Karen Troxler, PhD,#
El Gendler, MD, PhD,** and Lynne A. Opperman, PhD††

Purpose: Cranial defect reconstruction presents 2 challenges: induction of new bone formation, and providing structural support during the healing process. This study compares quantity and quality of new bone formation based on various materials and support frameworks.

Materials and Methods: Eighteen dogs underwent surgical removal of a significant portion of their cranial vault. Demineralized bone matrix was used to fill the defect in all animals. In 9 dogs, recombinant human bone morphogenetic protein-2 (rhBMP-2) was added, while the other 9 served as the non-rhBMP-2 group. In each group, 3 animals were fixed with cobalt chrome plates, 3 with adding platelet-rich plasma, and 3 fixed with a Lactosorb (Walter Lorenz Surgical, Inc, Jacksonville, FL) resorbable mesh. Necropsy was done at 12 weeks postoperative. Histomorphometry, density, and mechanical properties of the regenerate were analyzed.

Results: The non-rhBMP-2 groups showed minimal substitution of demineralized bone matrix with new bone, while only sporadic remnants of demineralized bone matrix were present in the rhBMP-2 groups. The defect showed more new bone formation ($P < .001$) and density ($P < .001$) in the rhBMP-2 groups by Kruskal-Wallis test. The area of new bone was not significantly different among the rhBMP-2 subgroups. The resorbable mesh struts showed no sign of bone invasion or substitution. In the non-rhBMP-2 resorbable mesh group, demineralized bone matrix almost totally disintegrated without replacement by new bone.

Conclusions: The addition of rhBMP-2 to demineralized bone matrix accelerated new bone formation in large cranial defects, regardless of the supporting framework or the addition of platelet-rich plasma. The use of a resorbable mesh in such defects is advisable only if rhBMP-2 is added.

© 2008 American Association of Oral and Maxillofacial Surgeons
J Oral Maxillofac Surg 66:277-285, 2008

*Assistant Professor, Department of Oral Biology and Maxillofacial Pathology, and the Department of Oral and Maxillofacial Surgery, School of Dentistry, Medical School of Georgia, Augusta, GA.

†Registrar, Department of Plastic, Reconstructive, and Aesthetic Surgery, KK Women's and Children's Hospital, Singapore.

‡Director, International Craniofacial Institute, and Cleft Lip and Palate Treatment Center, Medical City, Dallas, TX; and Adjunct Assistant Professor, Department of Biomedical Sciences, Baylor College of Dentistry, Texas A&M Health Science Center, Dallas, TX.

§Chairman, World Craniofacial Foundation, Dallas, TX; and Adjunct Professor, Department of Orthodontics, Baylor College of Dentistry, Texas A&M Health Science Center, Dallas, TX.

||Assistant Professor, Department of Anatomy, Division of Basic Medical Sciences, Mercer University School of Medicine, Macon, GA.

¶Medical Director, International Craniofacial Institute and Cleft Lip and Palate Treatment Center, Medical City, Dallas, TX.

#Biomet, Inc, Warsaw, IN.

**Professor Emeritus of Research Orthopaedics, University of Southern California, Los Angeles, CA; and President and Chief Executive Officer, Pacific Coast Tissue Bank, Los Angeles, CA.

††Associate Professor, Department of Biomedical Sciences, and Director of Technology Development, Baylor College of Dentistry, Texas A&M Health Science Center, Dallas, TX.

Presented at the Plastic Surgery Research Council Meeting 2005; the 10th International Congress on Cleft Palate and Related Craniofacial Anomalies 2005; and the 11th Biennial International Conference of the International Society of Craniofacial Surgery 2005.

Address correspondence and reprint requests to Dr Genecov: International Craniofacial Institute, Cleft Lip and Palate Treatment Center, 7777 Forest Lane, Suite C717, Dallas, TX 75230; e-mail: dggmd@craniofacial.net

© 2008 American Association of Oral and Maxillofacial Surgeons

0278-2391/08/6602-0012\$34.00/0

doi:10.1016/j.joms.2007.06.626

The use of demineralized bone matrix (DBM) as an allograft has been thoroughly investigated in cranial defect reconstruction.¹⁻⁶ However, using DBM sheets in very large skull defects raises many concerns. The rigidity of DBM by itself is not sufficient to protect the underlying brain until new bone is formed, which typically takes several months.⁴ The process may be accelerated by the addition of human recombinant bone morphogenetic protein-2 (rhBMP-2)⁷ or platelet-rich plasma (PRP).⁸ It is not currently possible to predict which factor, or combination of factors will produce the best results in a difficult reconstruction case, where the defect size is very large, the dura has matured, and adequate new bone formation is needed at a relatively early postoperative time point (12 weeks). Furthermore, the influence of the fixation method on bone induction by these factors is unknown.

The use of rigid internal metal fixation to support the DBM allograft necessitates a second surgery to remove the metal so it does not interfere with the growth and remodeling of the skull. Recently, several resorbable fixation materials have been introduced.⁹⁻¹⁷ Theoretically, these materials can maintain the skull vertex architecture, provide the necessary rigid protection, and prevent the encroachment of the soft tissues into the defect until the new bone is formed. As they are dissolved, these materials should permit their invasion and replacement by the new bone. A recent study showed that both resorbable and metal meshes worked well for long-term stability of phosphate cement used to fill large defects, but metal mesh was better for early stability, because the resorbable mesh group showed early delayed bone formation.¹⁸ It is possible that either rhBMP-2 or PRP used in combination with the resorbable materials could overcome this delay in bone formation, making the resorbable materials suitable for use where early stability is required, but where placement of metals would be difficult or inappropriate.

In this study, a cranial defect much larger than critical size was created in 18 adult dogs and combinations of the most commonly used reconstruction materials were tested. In addition to DBM, 2 supporting materials, cobalt chrome and Lactosorb (Walter Lorenz Surgical, Inc, Jacksonville, FL) mesh, the osteoinductive factor rhBMP-2, and the growth factor PRP, were used in various combinations in the reconstruction of the defects. At 12 weeks postoperatively, the histological and mechanical properties of the new bone created with each method were compared to one another, and to that of the surrounding normal bone.

We hypothesized that DBM would show early signs of osteoinduction and osteoconduction that would be augmented by the addition of rhBMP-2 or PRP. A

second hypothesis was that the resorbable mesh would demonstrate osteoconduction, disintegration, and invasion by new bone, which would also be accelerated by the addition of rhBMP-2 or PRP.

Materials and Methods

Eighteen adolescent, 9-month-old medical grade-2 male beagle dogs (mean age 9.17 months; range 9-10 months) underwent surgical removal of a significant portion of their cranial vault, creating a 2 cm long × 6 cm wide bone defect across the midline. The size of the defect was much larger than the critical size defect for dog calvaria.¹⁹ Two pieces of DBM (Pacific Coast Tissue Bank, Los Angeles, CA), 2 × 3 cm each, were used to fill the defect in each animal in all groups. The DBM was prepared from full-thickness cortical plates obtained from diaphyses of euthanized dog tibia. Lipids were extracted from the bone with 95% ethanol and ethyl ether and then demineralized in 0.6 N hydrochloric acid at 4°C. The bone was sterilized with ethylene oxide. The resultant sterilized pieces of DBM were then soaked in a solution of 500 ml of normal saline, 500 mg of vancomycin, 40 mg of gentamicin, and 1 g of cefazolin for at least half an hour prior to use. The ability of DBM used in this study to induce new bone formation has been tested in canine calvarial defects.⁴

The animals were randomly assigned to 2 groups, either with or without rhBMP-2. Each group was subdivided into 3 subgroups (3 animals each) according to the reconstruction protocol (detailed below). All animals tolerated the surgery and the postoperative period well and were sacrificed 12 weeks after the surgery. Density of the regenerate was measured and undecalcified sections from the defect were analyzed histomorphometrically. The housing, care, and experimental protocol were in accordance with guidelines established by the Institutional Animal Care and Research Advisory Committee at Medical City of Dallas (protocol number 04.05.2).

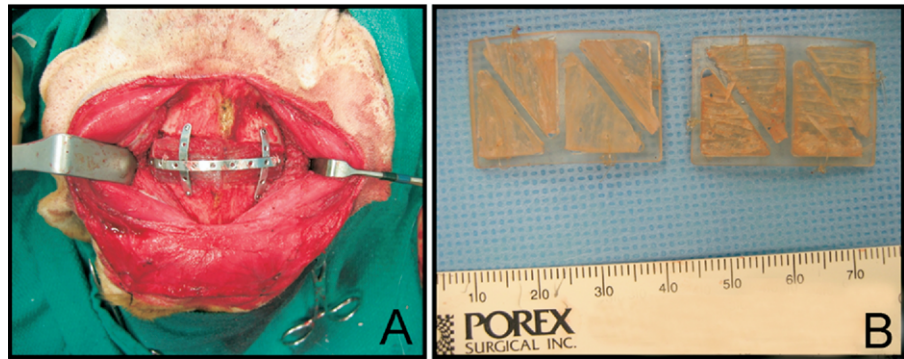
OPERATIVE PROCEDURE AND GROUP DESIGN

Under general anesthesia, the animals' heads were shaved, scrubbed with antiseptic solution, and draped. A bicoronal incision was made through the scalp, followed by subperiosteal dissection to expose the bone. The potential defect was then outlined on the bone so that it extended on both sides of the midline to measure 2 cm anteroposteriorly and 6 cm side-to-side. The calvarial defect was created by burring down along the markings.

In the first non-rhBMP-2 subgroup (group 1), the defect was bridged by 3 cobalt chrome plates in an H-shaped configuration (Fig 1A), and attached to the DBM sheets by resorbable sutures (Monocryl; Ethicon

FIGURE 1. Demineralized bone matrix (DBM) stabilization methods used in the reconstruction of canine cranial defects. *A*, Cranial defect, 2 × 6 cm, reconstructed with DBM and stabilized with cobalt chrome plates. *B*, Two segments of resorbable mesh framework filled with triangular DBM pieces were used to reconstruct the defect in groups 3 and 6. DBM was attached to resorbable mesh with nonresorbable sutures (Prolene; Ethicon Inc, Somersville, NJ).

Elsalanty et al. BMP2 in Cranial Defects Reconstruction. J Oral Maxillofac Surg 2008.



Inc, Somersville, NJ). In the second non-rhBMP-2 subgroup (group 2), the same stabilization method was used, but the DBM was enclosed between 2 layers of PRP. The PRP was prepared by harvesting autogenous blood under general anesthesia. A volume of 27 mL of autogenous blood was mixed with 3 mL of acid citrate dextrose solution-A for a final volume of 30 mL. This was then infused into the gravitational platelet separation system (GPS System; GP Supplies Limited, London, UK) and spun at 3,200 rpm for 12 minutes to separate 3 mL of PRP, which was aspirated into a syringe. A separate syringe was prepared, in which 5 mL of calcium chloride 10% was mixed with 5,000 U of thrombin. Using the GPS spray kit, both syringes were assembled and simultaneously pressed to spread out a layer of platelet-rich plasma, which coagulated when it came in contact with the thrombin-calcium chloride solution.

In the third non-rhBMP-2 subgroup (group 3), a custom-made rigid resorbable framework (Lactosorb) was used to stabilize the DBM (Fig 1B). Lactosorb is an 82:18 mixture of poly lactic and glycolic acids polymerized to ca 100 kDa polymer chains with a polydispersity of 2.2, and an inherent viscosity of 1.5 dL/g. Hydrolysis of the resorbable mesh progresses after implantation, and when the inherent viscosity reaches 0.7 dL/g from week 6 to 12, its strength weakens rapidly, and continues, reaching 0 strength by about 12 to 15 weeks postimplantation. Complete resorption of the mesh ranges from 9 to 15 months after surgery.¹⁵ The triangular spaces within the resorbable mesh were filled with DBM chips of the same shape and they were fixed together and to the surrounding bone by nonresorbable sutures (Prolene, Ethicon Inc). Then, the resorbable mesh-DBM complex, enclosed between 2 layers of PRP, was tightly fitted into the defect.

Similarly, in the first rhBMP-2 subgroup (group 4), 3 cobalt chrome plates were used to stabilize the DBM. However, the DBM was positioned on top of a layer of type I bovine absorbable collagen sponge soaked with rhBMP-2 (Helistat; Integra LifeSciences Corporation, Plainsboro, NJ) separating it from the underlying dura. The concentration of rhBMP-2 was 0.4 mg/mL

and each sponge was infused with 1.4 mL of solution, which was equivalent to 0.56 mg of rhBMP-2. The sponge was soaked with rhBMP-2 for at least 15 minutes prior to implantation on top of the dura. In the second rhBMP-2 subgroup (group 5), a layer of PRP was first laid on the surface of the dura, followed by a layer of rhBMP-2-soaked sponge, and then the DBM was positioned on top of the rhBMP-2 layer and stabilized by cobalt chrome plates, and covered by a second layer of PRP. In the third rhBMP-2 subgroup (group 6), a resorbable mesh framework was used to stabilize the DBM as in group 3, but the resorbable mesh-DBM complex was positioned on top of an rhBMP-2-soaked collagen sponge. A summary of the treatment protocol in the 6 groups is outlined in Table 1. The surgical wound was closed in layers.

Preanesthesia medications given were subcutaneous or intramuscular 0.01 mg/kg glycopyrrolate, 0.2 mg/kg midazolam, 0.2 mg/kg hydromorphone, and 6 mg/kg gentamicin. Induction of anesthesia was obtained with sevoflurane and oxygen via mask. The dogs were intubated and maintained on isoflurane 1.5% to 3.5%, and oxygen. Perioperatively, intravenous methylprednisolone 30 mg/kg was given as the calvarial defects were made. Postoperatively, at 4 to 6 hours, intravenous methylprednisolone 15 mg/kg, hydromorphone 0.2 mg/kg was administered, then, as needed midazolam 0.1 to 0.3 mg/kg per hour for 2 hours, and subcutaneous gentamicin 6 mg/kg was given for 5 days.

SAMPLE COLLECTION AND PREPARATION

At necropsy, each bone defect was explored and a rectangle of bone was excised, including the area of the defect surrounded by a frame of host bone, and immediately immersed in 10% formaldehyde. Two weeks later, samples were taken and assigned for either mechanical or histological examination. To assess the density and material properties of the bone regenerate, a protocol similar to one used previously was used.²⁰⁻²³ During preparation, sites were marked with a graphite line indicating a reference line noting

Table 1. HISTOMORPHOMETRIC ANALYSIS OF RECONSTRUCTED CRANIAL DEFECTS

Group	Description	Bone Area (%) [*]	Reg Min	Reg Max	Cort Thick	D/C (%)
1	DBM + Cobalt	8.21 ± 3.1	†	†	0	-
2	DBM + PRP + Cobalt	8.35 ± 2.7	†	†	0	-
3	DBM + PRP + Lactosorb‡	7.8 ± 4.43	†	†	0	-
4	DBM + rhBMP-2 + Cobalt	50.19 ± 9.31	2.22 ± 0.66	5.47 ± 2.01	479.99 ± 74.75	126.38 ± 67.38
5	DBM + rhBMP-2 + Cobalt + PRP	48 ± 4.6	3.09 ± 0.09	6.07 ± 0.8	467.68 ± 25.91	142.34 ± 38.14
6	DBM + rhBMP-2 + Lactosorb	37.72 ± 10.04	1.79 ± 0.91	3.33 ± 1.08	522.45 ± 145.82	82.86 ± 32.38

NOTE. Maximum (Max) and minimum (Min) regenerate (Reg) thickness, maximum cortical thickness (Cort Thick) in new bone, and percent defect filled with bone compared with control (D/C). All values are expressed as mean ± SD.

Abbreviations: DBM, demineralized bone matrix; PRP, platelet-rich plasma; rhBMP-2, recombinant human bone morphogenetic protein-2.

^{*}Percentage of bone area in the reconstructed defect.

†Too minimal and variable to measure reliably.

‡Walter Lorenz Surgical, Inc, Jacksonville, FL.

Elsalanty et al. *BMP2 in Cranial Defects Reconstruction. J Oral Maxillofac Surg* 2008.

the anatomical long axis of the specimen. Bone strips and cylinders were harvested from the cortex using a Dremel 732 Heavy Duty Flex Shaft Rotary Tool (Dremel North America, Racine, WI) and 6.0 mm inner-diameter trephine burrs (Ace Surgical Supply, Inc, Brockton, MA). Cooling was maintained with a water drip. Specimens were stored in a solution of 95% ethanol and isotonic saline in equal proportions. This media has been shown to maintain the elastic properties of cortical bone over time.^{24,25}

A digital caliper was used to measure the specimen dimensions to the nearest 0.01 mm. Moist weights of the specimens were obtained on a Mettler PM460 analytical balance (Mettler-Toledo Inc, Columbus, OH) reading to the nearest 0.01 g. Submerged weights were obtained using a Mettler suspension jig (Mettler-Toledo Inc). Apparent density calculations were based on Archimedes' principle of buoyancy²⁶ and the formula: density (gm/cm³) = (dry weight/[dry weight - wet weight]) × 0.997.

ULTRASOUND ASSESSMENT OF MATERIAL PROPERTIES

Longitudinal ultrasonic waves were generated by Panametrics V312-N-SU transducers (Olympus NDT, Houston, TX) resonating at 10 MHz. The transducers were powered with a Hewlett Packard Model 214A pulse generator (Hewlett Packard, Palo Alto, CA). Pulse delays induced by passage of ultrasonic waves through the bone were read on a Tektronix TDS420 digitizing oscilloscope (Tektronix Texas, LLC, Richardson, TX). The bone cylinder was mounted on a 4-in Rotary Table P/N 3700, (Sherline Products, Inc, Vista, CA), which allowed accurate rotations for a 360° turn. Pulse delays for each specimen were measured in 22.5° angular intervals up to 180°. Ultrasonic velocities were calculated by dividing the specimen thickness or diameter by the recorded time delay

minus the standard system delay. To minimize error, all measurements were repeated twice, and the mean value of the 2 measurements was used for analysis. Samples which gave readings with inconsistencies greater than 5% were discarded.

A refined method of determining the axes of minimum and maximum stiffness in the plane of the cortical plate was used.²⁶ A program written in Mathcad (version 2001, Mathsoft Engineering & Education, Inc, Cambridge, MA) was used to fit the calculated longitudinal velocities and their angular orientation for each bone specimen to a sine function (a · sin [X + b] + c). The coefficients a, b, and c corresponded to the orientation of the axes of maximum stiffness, the average velocity, and the maximum deviation of the curve from the average velocity. The direction of the axis of maximum stiffness corresponded to the direction of peak longitudinal velocity. Likewise, the minimal principal axis, or least stiffness direction, corresponded to the lowest velocity. The third axis was always tangential or perpendicular to the cortical plane.^{22-24,27}

Correlation coefficients were generated and tested for significance for each plot between measured values and the idealized sine curve as generated by the sinfit function. For specimens that showed larger deviations from the sine functions, we examined the curves to assess if they were symmetrical, whether they had broad peaks and troughs, and whether the peaks and troughs maintained a 90° separation from each other. After 3 axes were determined in the cortical bone plates, the measurements of transverse velocities were conducted on 3 planes formed by them.

Elastic properties were calculated from elastic coefficients; the latter were derived from cortical density and the longitudinal and transverse velocities based on the principles of the linear elastic wave

theory and Hooke's law.^{24,28} Briefly, the elastic modulus (E) measures axial stiffness or the amount of deformation (strain) relative to an applied load (stress). Subscripts, as in E_1 , E_2 , or E_3 , indicate the appropriate axis for each elastic modulus. E_1 , E_2 , and E_3 are elastic moduli along different axes. Similarly, the subscripts indicate orientation for shear moduli and Poisson's ratios. Shear modulus (G) measures stiffness in shear or angular deformation relative to applied shearing loads in a plane between 2 axes indicated by the subscripts (G_{12} , G_{31} , or G_{32}). Poisson's ratio (ν) is a measure of stiffness of a structure perpendicular to that of the applied load. It is a ratio of the strain in the secondary direction (response direction) divided by strain in the primary direction (applied load direction). The first subscript indicates the axis of the applied load and the second subscript indicates the response direction as in ν_{12} , ν_{13} , ν_{21} , ν_{23} , ν_{31} , and ν_{32} . In our study, elastic properties were calculated from original data such as density and ultrasonic velocities, using a program written in Mathcad (Version 11.0, Mathsoft Engineering & Education, Inc). Ultrasonic velocities and densities were used to calculate 6×6 matrices, or "C" matrices, including 9 unique elastic coefficients (C_{11} , C_{22} , C_{33} , C_{44} , C_{55} , C_{66} , C_{12} , C_{13} , and C_{23}) and then 12 technical constants (3 elastic moduli – E_1 , E_2 , E_3 ; 3 shear moduli – G_{12} , G_{31} , G_{23} , and 6 Poisson's ratios – ν_{12} , ν_{21} , ν_{13} , ν_{31} , ν_{23} , ν_{32}). A consequence of the assumption of orthotropic material symmetry is that $\nu_{ji}E_i = \nu_{ij}E_j$. Thus, Poisson's ratios can be simplified and presented as 3, rather than 6 values. These are given here as ν_{12} , ν_{13} , and ν_{23} . We also compared relative stiffness between axes by using ratios of elastic constants, such as E_1/E_2 , E_1/E_3 , E_2/E_3 to quantify anisotropy in 3 cortical planes.

The error of this ultrasonic method has been assessed using repeated measurements,²⁶ and was 2.1% for the longitudinal velocities and 3.1% for the transverse velocities. For the individual sites, measurement error was assessed by calculating the percentage ratio between the variance of the method error (squared Dahlberg's error) and the population variance of that measurement (squared standard deviation). For the longitudinal velocities, the error percentage was always less than 8.3% of the total biological variance; and for transverse velocities, the error percentage was always less than 13.3% of the total biological variance.

HISTOLOGY AND HISTOMORPHOMETRY

From each animal, 2 samples were assigned for undecalcified sectioning, and were embedded in methylmethacrylate, sectioned at $75 \mu\text{m}$ and stained with Stevenel's blue. Tissue specimens from each animal were assigned for histomorphometry. Digital

photographs were taken at $2.5\times$ magnification using Spot software, version 4.0.8 (Diagnostic Instruments, Inc, Sterling Heights, MI), with a Kodak color video camera (Eastman Kodak Co, Rochester, NY) mounted on a Zeiss Axioplan microscope (Carl Zeiss MicroImaging, Inc, Thornwood, NY). Area measurements were taken using Metamorph software version 6.2r2 (Molecular Devices, Inc, Sunnyvale, CA) on an average of 13 fields per animal, spanning the region of the reconstructed defect. After calibration, the total tissue area and the nonbone areas were measured. The bone area was calculated as the difference between the total tissue area and the sum of nonbone areas. For comparisons, the percentage of the new bone area to the total tissue area was used.

STATISTICAL ANALYSIS

Statistical analysis was carried out using SPSS software version 12 (SPSS, Inc, Chicago, IL). The histomorphometry and bone density data were tested using nonparametric Kruskal-Wallis and Mann-Whitney tests. The ultrasound data were analyzed using the Minitab statistical analysis program 14.1 (Minitab, Inc, State College, PA). Descriptive statistics, including means, standard deviations, and standard error of means, were calculated for all measurements. Significance levels were set at $\alpha = 0.05$.

Results

HISTOLOGY

Groups 1 and 2 (cobalt and DBM, and cobalt, DBM, and PRP, respectively) showed only minimal substitution of DBM with new bone, mainly at the bone-DBM interface. Sporadic islands of new bone within the DBM could be identified in some sections; otherwise the DBM remained almost intact with little evidence of disintegration, substitution, or bone apposition at the dural or galeal surfaces (Fig 2). In group 3 (DBM, stabilized with resorbable mesh), DBM disintegration was much more profound (Fig 2). However, similar to the first 2 groups, there was minimal new bone formation, which was localized at the bone-DBM interface with no evidence of new bone apposition on the surfaces of the resorbable mesh struts. The resorbable mesh surfaces showed no evidence of resorption and were surrounded by a frame of fibrous tissue, separating it from the disintegrating DBM. Interestingly, considerable aggregation of muscle tissue, not evident in the other 2 non-rhBMP-2 groups, was identified and tended to correlate with the locations of resorbable mesh.

In contrast, all sections from the rhBMP-2 groups (groups 4, 5, and 6) showed new bone formation, with only sporadic remnants of DBM identified (Fig 2). The

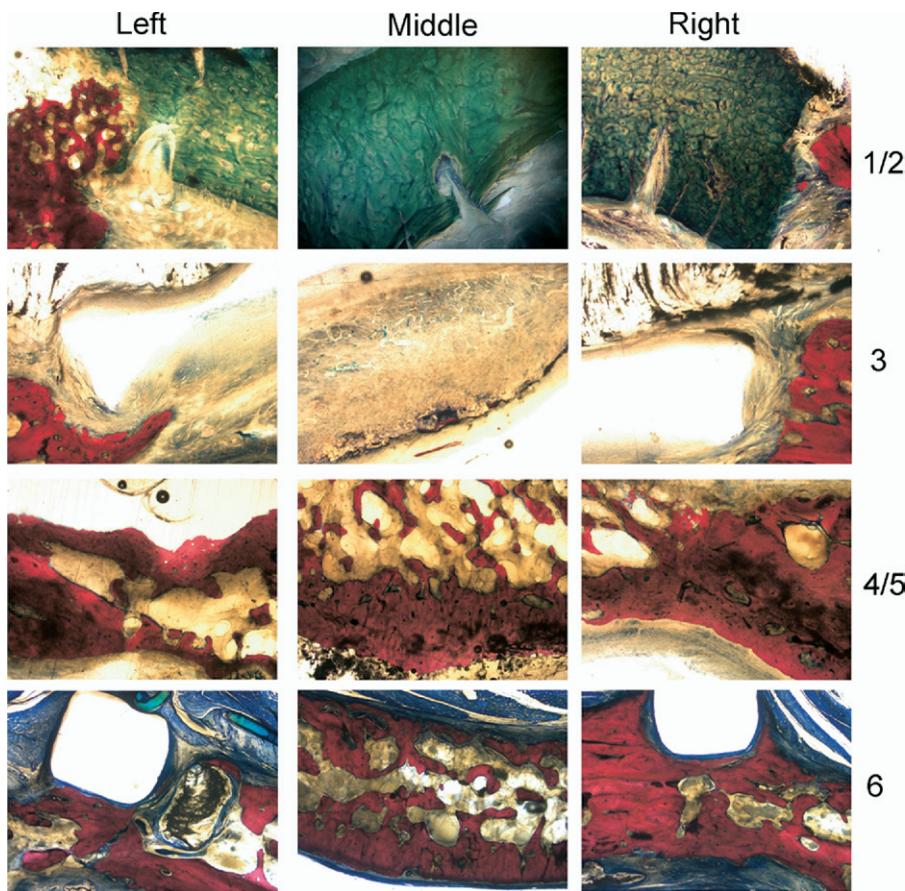


FIGURE 2. Photomicrographs of undecalcified histological sections through representative reconstructed cranial defects from each group. Because the results in groups 1 and 2 and in groups 4 and 5 were similar, a single sample is shown to represent groups 1 and 2, and another for groups 4 and 5. From left to right the micrographs show sections of the left host/graft boundary, the middle of the grafted region, and the right edge of the host/graph boundary. Groups 1 and 2 (1/2) show only minimal demineralized bone matrix (DBM) (dark green) disintegration and substitution by new bone at the left edge (red, mineralized woven bone). Group 3 (3) shows almost total DBM disintegration. Spaces that were occupied by resorbable mesh struts can be seen at both the right and left ends. Groups 4 and 5 (4/5) show almost no sign of remaining DBM. New bone spanned the defect with condensed bone spanning the outer and inner cortices. Group 6 (6) shows similar pattern of bone formation as in groups 4 and 5; however, resorbable mesh spaces were still well defined and surrounded by capsules of fibrous tissue with no sign of invasion by new bone. Aggregation of muscle tissue (blue) can also be seen in most sections in this group. This accumulation of muscle was not seen in the other groups. Magnification $\times 2.5$.

Elsalanty et al. BMP2 in Cranial Defects Reconstruction. J Oral Maxillofac Surg 2008.

bone-defect interface was no longer recognizable. New bone was more condensed along the galeal and dural surfaces, forming outer and inner cortical plates separated by an intermediate area of trabecular bone of variable thickness. In group 6 (rhBMP-2, resorbable mesh, and DBM), there was no evidence of mesh resorption or tissue invasion (Fig 2). Instead, each strut was surrounded by a fibrous tissue envelope. As in group 3, there was a marked aggregation of muscle tissue at the resorbable mesh locations.

HISTOMORPHOMETRY

The reconstructed zone showed more new bone formation ($P < .001$) in the rhBMP-2 groups than the non-rhBMP-2 groups, by Kruskal-Wallis test (Fig 3). In the rhBMP-2 groups, the maximum bone regenerate thickness tended to correlate with the locations of the cobalt chrome struts in groups 4 and 5 and away from the resorbable mesh struts in group 6. The total percent area of new bone formation, maximum and minimum bone regenerate thickness, cortical thickness, and regenerate to control thickness ratio were not significantly different among the 3 rhBMP-2 subgroups. However, except for cortical thickness, the resorbable mesh group (group 6) consistently had the lowest values (Table 1).

TISSUE DENSITY

No difference in density was detected between control host bone of the rhBMP-2 and non-rhBMP-2 groups ($P = .530$). In both groups, the difference between the control and defect bone was significant ($P < .001$). However, the rhBMP-2 group had higher density in the reconstructed defect than the non-rhBMP-2 group (1.184 mg/cm^3 versus 1.150 mg/cm^3 ; $P < .001$). The average tissue density in the reconstructed zone of the rhBMP-2 groups reached 87.3% of the average density of the control bone in the same animals, compared with 61.8% in the non-rhBMP-2 groups ($P < .0001$). No significant differences were found between the 3 non-rhBMP-2 groups, or between the 3 rhBMP-2 subgroups.

BONE ELASTIC PROPERTIES

The control bone of the non-rhBMP-2 and rhBMP-2 groups had similar bone elastic properties, while the bone of the reconstructed zone in the rhBMP-2 group had higher bone elastic (E) and shear (G) stiffness than in the non-rhBMP-2 group ($P < .001$; Table 2). The rhBMP-2 and non-rhBMP-2 groups had different Poisson's ratio in ν_{13} ($P = .021$). This indicates that the rhBMP-2 group had more anisotropy than the non-rhBMP-2 group. The stiffness of the reconstructed bone

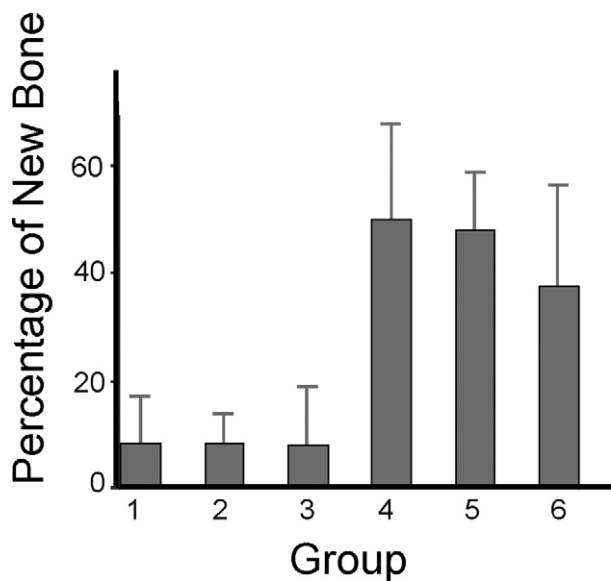


FIGURE 3. Graph showing the differences between groups in the percentage of new bone formed within the reconstructed cranial defects. The reconstructed zone showed more new bone formation ($P < .001$) in the recombinant human bone morphogenetic protein-2 (rhBMP-2) groups than the non-rhBMP-2 groups, by Kruskal-Wallis test.

Elsalanty et al. *BMP2 in Cranial Defects Reconstruction. J Oral Maxillofac Surg* 2008.

was around 24% of the control bone in the non-rhBMP-2 group, compared with 60% in the rhBMP-2 group.

Discussion

Numerous studies have documented the effectiveness of DBM in the reconstruction of critical size

cranial defects.^{1,2,4,5,29} The osteoinductive and osteoconductive abilities of the DBM used in this study has previously been tested in rabbit subcutaneous tissues,³⁰ canine calvarial defects,⁴ and in human patients.^{5,29} Clinically, however, adequate new bone formation in huge and subtotal cranial defects could take several months to be established, sometimes with inconsistent mineralization.^{1,5} This was especially observed in the absence of immature dura lining the defect. This study aimed at identifying the fixation and bone augmentation method that produces the most adequate bone under 3 conditions: defect size much larger than the critical size, a relatively early time point of 3 months postoperative, and with mature dura mater lining the defect.

In the non-rhBMP-2 groups, replacement of DBM by new bone was still in the early stages at 12 weeks postoperative. Disintegration and replacement of DBM by new bone formation seemed to start primarily at the bone-DBM interface, and to a lesser extent at the dural surfaces. The lack of osteogenesis at the dural surface can be attributed to the maturity of the dura in these animals. It has been well documented that the dura loses much of its osteogenic ability after skeletal maturation.³¹⁻³⁴ Neither the method of fixation nor the addition of PRP appeared to accelerate osteogenesis in these groups.

The resorbable mesh group showed marked resorption of DBM, which may have been caused by the acidity of the resorbable mesh implants. The resorbable mesh struts themselves were morphologically intact with no sign of infiltration or substitution. Fur-

Table 2. BONE REGENERATE ELASTIC PROPERTIES OF THE RECONSTRUCTED DEFECTS IN THE RHBMP-2 VERSUS NON-RHBMP-2 GROUPS

	Non-rhBMP-2				rhBMP-2				ANOVA*	
	Defect (n = 8)		Control (n = 5)		Defect (n = 4)		Control (n = 3)		F	P
	Mean	SD	Mean	SD	Mean	SD	Mean	SD		
E ₁ (GPa)	3.0	0.2	9.8	0.9	7.1	1.8	11.8	2.7	48.3	< .001
E ₂ (GPa)	2.9	0.1	11.4	0.9	7.5	1.5	12.3	2.4	81.1	< .001
E ₃ (GPa)	3.3	0.3	18.2	1.8	9.5	1.6	16.1	2.9	131.0	< .001
G ₁₂ (GPa)	1.1	0.1	3.7	0.4	2.8	0.6	4.5	1.0	67.8	< .001
G ₃₁ (GPa)	1.2	0.1	5.7	0.5	3.4	0.5	5.6	0.8	186.6	< .001
G ₂₃ (GPa)	1.2	0.1	6.1	0.8	3.5	0.6	5.9	1.0	120.8	< .001
ν ₁₂	0.31	0.05	0.40	0.08	0.29	0.11	0.32	0.04	0.21	NS
ν ₁₃	0.30	0.08	0.09	0.11	0.17	0.09	0.18	0.09	7.54	.021
ν ₂₃	0.25	0.02	0.18	0.08	0.20	0.11	0.17	0.04	1.66	NS
E ₂ /E ₃	0.89	0.05	0.63	0.07	0.79	0.08	0.76	0.04	7.01	.024

NOTE. Subscripts, as in E₁, E₂, or E₃, indicate the appropriate axis for each elastic modulus (E). Shear modulus (G) measures stiffness in shear or angular deformation relative to applied shearing loads in a plane between 2 axes indicated by the subscripts (G₁₂, G₃₁, or G₃₂). Poisson's ratio (ν) is a measure of stiffness of a structure perpendicular to that of the applied load. The first subscript indicates the axis of the applied load and the second subscript indicates the response direction as in ν₁₂, ν₁₃, and ν₂₃.

rhBMP-2, recombinant human bone morphogenetic protein-2.

*Values from samples of the reconstructed defect in the non-rhBMP-2 groups were compared with those from rhBMP-2 groups.

Elsalanty et al. *BMP2 in Cranial Defects Reconstruction. J Oral Maxillofac Surg* 2008.

ther research is required to explain the interaction between resorbable mesh implants and DBM.

During reconstruction, resorbable mesh should function as an osteoconductive space filler that provides structural support and protection for the underlying brain during bone healing.³⁵ Ideally, it should have porosity to allow for cell infiltration; and the rate of new bone formation should be comparable to the rate of carrier degradation so that the mechanical integrity is not compromised.³⁵ According to our results, the rate of resorbable mesh degradation and substitution by new bone was much slower than that of DBM degradation. Knowing that resorbable mesh loses almost all of its strength at 12 weeks,¹⁵ we can assume that degradation of DBM in this case would leave the reconstructed zone virtually unprotected until adequate new bone is formed, which may take several months.⁴

On the other hand, all the rhBMP-2 groups showed accelerated new bone formation within the defects compared with the non-rhBMP-2 groups. The architecture of the new bone was similar to the normal calvarial bone, evident both histologically and by the increase in anisotropy. Although the amount of new bone and the cortical thickness were not affected by the method of fixation, cobalt chrome struts showed more osteoconduction than resorbable mesh, as the latter was always separated from the new bone by an envelope of fibrous tissue. Overall, both the amount and the quality of osteogenesis at 12 weeks were dependent primarily on rhBMP2, regardless of the method of fixation or the addition of PRP.

It has been reported that PRP promotes angiogenesis and osteogenesis via the presence of growth factors which include platelet derived growth factor, platelet-derived endothelial cell growth factor, and transforming growth factor- β .³⁶⁻³⁸ Kim et al reported that demineralized bone and PRP produced a significantly higher percentage of bone regeneration as compared with the use of demineralized bone alone.³⁹ However, Marden et al found that platelet-derived growth factor inhibited bone regeneration induced by osteogenin, a bone morphogenetic protein, in rat craniotomy defects.⁴⁰ In the present study, there was no evidence that PRP either promotes or interferes with osteogenesis occurring in the presence of rhBMP-2.

Stiffness of new bone within the reconstructed zone in the rhBMP-2 group was more than twice that of bone in the non-rhBMP-2 group. The rhBMP-2-synthesized bone was anisotropic, resembling normal calvarial bone, compared with the relatively isotropic DBM.

Based on extensive previous research and clinical experience, we believe that cranial defects can be reconstructed by DBM alone, if enough time is given

for DBM substitution by new bone formation. This process can be slow, especially in the absence of the primary pool for osteogenic cells, the immature dura, in which case, most of the new bone will generate at the interface between the host bone and the defect edge. In this study, however, acceleration of bone formation and maturation produced by adding rhBMP-2 to DBM was significant. rhBMP-2 is now becoming more accepted as a standard component in spinal fusion surgery,⁴¹⁻⁴⁵ and it has similar potential in cranial reconstruction. This potential becomes even more relevant whenever super-size and subtotal cranial defects need to be reconstructed so that permanent brain protection is achieved as early as possible.

Although we have found no evidence that the method of fixation affected new bone formation, other factors may decide the appropriate method for each patient. Cobalt chrome needs to be removed in a later surgery so as not to interfere with skull remodeling in growing patients. On the other hand, resorbable mesh does not require removal, but it can only be structurally supportive during the first few weeks after surgery.

Rigidity of the supporting framework is particularly critical in huge and subtotal cranial defects. Therefore, it is advisable to add rhBMP-2 whenever resorbable mesh is used in such defects, so that enough bone is generated before resorbable mesh loses its stiffness. Otherwise, it may be safer to maintain rigid fixation of the DBM with nonosseointegrated, non-resorbable internal fixation material, like cobalt chrome, until proper bone is formed, if secondary surgery to remove the hardware several months later is feasible.

In conclusion, rhBMP-2 accelerated the osteoinductive effect of DBM in large cranial defects, regardless of the supporting framework. Adding PRP did not influence the regeneration process whether rhBMP-2 was used or not. The use of resorbable mesh in super-size cranial defects is advisable only if rhBMP-2 is added to enhance early bone formation.

References

1. Chen TM, Wang HJ: Cranioplasty using allogeneic perforated demineralized bone matrix with autogenous bone paste. *Ann Plast Surg* 49:272, 277, 2002
2. Moss SD, Joganic E, Manwaring KH, et al: Transplanted demineralized bone graft in cranial reconstructive surgery. *Pediatr Neurosurg* 23:199, 204, 1995
3. Neigel JM, Ruzicka PO: Use of demineralized bone implants in orbital and craniofacial reconstruction and a review of the literature. *Ophthal Plast Reconstr Surg* 12:108, 1996
4. Salyer KE, Bardach J, Squier CA, et al: Cranioplasty in the growing canine skull using demineralized perforated bone. *Plast Reconstr Surg* 96:770, 1995
5. Salyer KE, Gendler E, Menendez JL, et al: Demineralized perforated bone implants in craniofacial surgery. *J Craniofac Surg* 3:55, 1992

6. Schmitz JP, Hollinger JO: A preliminary study of the osteogenic potential of a biodegradable alloplastic-osteoinductive alloimplant. *Clin Orthop Relat Res* 237:245, 1988
7. Schwartz Z, Somers A, Mellonig JT, et al: Addition of human recombinant bone morphogenetic protein-2 to inactive commercial human demineralized freeze-dried bone allograft makes an effective composite bone inductive implant material. *J Periodontol* 69:1337, 1998
8. Marx RE, Carlson ER, Eichstaedt RM, et al: Platelet-rich plasma: Growth factor enhancement for bone grafts. *Oral Surg Oral Med Oral Pathol Oral Radiol Endod* 85:638, 1998
9. Ashammakhi N, Peltoniemi H, Waris E, et al: Developments in craniomaxillofacial surgery: Use of self-reinforced bioabsorbable osteofixation devices. *Plast Reconstr Surg* 108:167, 2001
10. Bondre S, Lewandowski KU, Hasirci V, et al: Biodegradable foam coating of cortical allografts. *Tissue Eng* 6:217, 2000
11. Bostman O, Pihlajamaki H: Clinical biocompatibility of biodegradable orthopaedic implants for internal fixation: A review. *Biomaterials* 21:2615, 2000
12. Boyan BD, Lohmann CH, Somers A, et al: Potential of porous poly-D,L-lactide-co-glycolide particles as a carrier for recombinant human bone morphogenetic protein-2 during osteoinduction in vivo. *J Biomed Mater Res* 46:51, 1999
13. Bozic KJ, Perez LE, Wilson DR, et al: Mechanical testing of bioresorbable implants for use in metacarpal fracture fixation. *J Hand Surg [Am]* 26:755, 2001
14. Eppley BL: Use of resorbable plates and screws in pediatric facial fractures. *J Oral Maxillofac Surg* 63:385, 2005
15. Eppley BL, Morales L, Wood R, et al: Resorbable PLLA-PGA plate and screw fixation in pediatric craniofacial surgery: Clinical experience in 1883 patients. *Plast Reconstr Surg*. 114: 850,857, 2004
16. Ewers R, Lieb-Skowron J: Bioabsorbable osteosynthesis materials. *Facial Plast Surg* 7:206, 1990
17. Gogolewski S: Resorbable polymers for internal fixation. *Clin Mater* 10:13, 1992
18. Kremer M, Butsch M, Schnell M, et al: Miniaturized mechatronic distraction plate for unidirectional internal distraction: Technical concepts, design features and preliminary experimental results. *Proceedings of the 3rd International Congress of Craniofacial and Maxillofacial Distraction*; Paris, France, 2001
19. Schmitz JP, Hollinger JO: The critical size defect as an experimental model for craniomandibulofacial nonunions. *Clin Orthop Relat Res* 205:299, 1986
20. Peterson J, Dechow PC: Material properties of the inner and outer cortical tables of the human parietal bone. *Anat Rec* 268:7, 2002
21. Peterson J, Dechow PC: Material properties of the human cranial vault and zygoma. *Anat Rec A Discov Mol Cell Evol Biol* 274:785, 2003
22. Schwartz-Dabney CL, Dechow PC: Accuracy of elastic property measurement in mandibular cortical bone is improved by using cylindrical specimens. *J Biomech Eng* 124:714, 2002
23. Schwartz-Dabney CL, Dechow PC: Variations in cortical material properties throughout the human dentate mandible. *Am J Phys Anthropol* 120:252, 2003
24. Ashman RB, Cowin SC, Van Buskirk WC, et al: A continuous wave technique for the measurement of the elastic properties of cortical bone. *J Biomech* 17:349, 1984
25. Zioupos P, Smith C, An Y: Factors affecting mechanical properties of bone, *in* An Y, Draughn R (eds): *Mechanical Testing of Bone and the Bone-Implant Interface*. Boca Raton, FL, CRC Press, 1999, p 87
26. Wang Q, Dechow PC: Elastic properties of external cortical bone in the craniofacial skeleton of the rhesus monkey. *Am J Phys Anthropol* 131:402, 2006
27. Yoon HS, Katz JL: Ultrasonic wave propagation in human cortical bone-II. Measurements of elastic properties and microhardness. *J Biomech* 9:459, 1976
28. Dechow PC, Nail GA, Schwartz-Dabney CL, et al: Elastic properties of human supraorbital and mandibular bone. *Am J Phys Anthropol* 90:291, 1993
29. Salyer KE, Gendler E, Squier CA: Long-term outcome of extensive skull reconstruction using demineralized perforated bone in Siamese twins joined at the skull vertex. *Plast Reconstr Surg* 99:1721, 1997
30. Gendler E: Perforated demineralized bone matrix: A new form of osteoinductive biomaterial. *J Biomed Mater Res* 20:687, 1986
31. Greenwald JA, Mehrara BJ, Spector JA, et al: Biomolecular mechanisms of calvarial bone induction: Immature versus mature dura mater. *Plast Reconstr Surg* 105:1382, 2000
32. Greenwald JA, Mehrara BJ, Spector JA, et al: Immature versus mature dura mater: II. Differential expression of genes important to calvarial reossification. *Plast Reconstr Surg* 106:630, 2000
33. Gosain AK, Santoro TD, Song LS, et al: Osteogenesis in calvarial defects: Contribution of the dura, the pericranium, and the surrounding bone in adult versus infant animals. *Plast Reconstr Surg* 112:515, 2003
34. Hobar PC, Schreiber JS, McCarthy JG, et al: The role of the dura in cranial bone regeneration in the immature animal. *Plast Reconstr Surg* 92:405, 1993
35. Li G, Bouxsein ML, Luppen C, et al: Bone consolidation is enhanced by rhBMP-2 in a rabbit model of distraction osteogenesis. *J Orthop Res* 20:779, 2002
36. Okuda K, Kawase T, Momose M, et al: Platelet-rich plasma contains high levels of platelet-derived growth factor and transforming growth factor-beta and modulates the proliferation of periodontally related cells in vitro. *J Periodontol* 74:849, 2003
37. Weibrich G, Kleis WK, Hafner G, et al: Growth factor levels in platelet-rich plasma and correlations with donor age, sex, and platelet count. *J Craniomaxillofac Surg* 30:97, 2002
38. Zhang CQ, Yuan T, Zeng BF: Experimental study of the effect of platelet-rich plasma on osteogenesis in rabbit. *Chin Med J (Engl)* 117:1853, 2004
39. Kim SG, Kim WK, Park JC, et al: A comparative study of osseointegration of Avana implants in a demineralized freeze-dried bone alone or with platelet-rich plasma. *J Oral Maxillofac Surg* 60:1018, 2002
40. Marden LJ, Fan RS, Pierce GF, et al: Platelet-derived growth factor inhibits bone regeneration induced by osteogenin, a bone morphogenetic protein, in rat craniotomy defects. *J Clin Invest* 92:2897, 1993
41. Helm GA, Alden TD, Sheehan JP, et al: Bone morphogenetic proteins and bone morphogenetic protein gene therapy in neurological surgery: A review. *Neurosurgery* 46:1213, 2000
42. Khan SN, Lane JM: The use of recombinant human bone morphogenetic protein-2 (rhBMP-2) in orthopaedic applications. *Expert Opin Biol Ther* 4:741, 2004
43. McKay B, Sandhu HS: Use of recombinant human bone morphogenetic protein-2 in spinal fusion applications. *Spine* 16: S66, 2002
44. Szpalski M, Gunzburg R: Recombinant human bone morphogenetic protein-2: A novel osteoinductive alternative to autogenous bone graft? *Acta Orthop Belg* 71:133, 2005
45. Zlotolow DA, Vaccaro AR, Salamon ML, et al: The role of human bone morphogenetic proteins in spinal fusion. *J Am Acad Orthop Surg* 8:3, 2000